Comparison of Model Predictive Control Performance Using Grey-Box and White-Box Controller Models of a Multi-zone Office Building

Damien PICARD[1*], Maarten SOURBRON[1], Filip JORISSEN[1], Zdeněk VÁŇA[2], Jiří CIGLER[2], Lukás FERKL[3], Lieve HELSEN[1,4]

[1] KU Leuven, Department of Mechanical Engineering,
Leuven, Belgium
damien.picard@kuleuven.be

[2] Feramat Cybernetics s.r.o.,
Prague, Czech Republic

[3] University Centre for Energy Efficient Buildings, Czech Technical University,
Prague, Czech Republic

[4] EnergyVille,
Waterschei, Belgium
* Corresponding Author

ABSTRACT

Model Predictive Control (MPC) is a promising control method to reduce the energy use of buildings. Its commercialization is, however, hampered by the difficulty of obtaining a reliable controller model. This paper compares two approaches to obtain such controller model: (1) a white-box model approach for which a detailed first-principles building model is linearized, and (2) a system identification method using a grey-box model approach. The MPC performance using both model approaches is evaluated on a validated 12 zones model of an existing office building. The results indicate that the MPC performance is very sensitive to the prediction accuracy of the controller model. This paper shows that both approaches can lead to an efficient MPC as long as very accurate identification data sets are available. For the considered simulation case, the white-box MPC resulted in a better thermal comfort and used only 50% of the energy used by the best grey-box MPC.

1. INTRODUCTION

Model based Predictive Control (MPC) is a control technique for dynamic systems that computes optimal control set points in order to minimize a predefined cost. For this, the controller contains a dynamic model of the system that is used in an optimization routine that solves at each control step an optimal control problem (Maciejowski, 2002). Building HVAC systems present an interesting application for MPC, especially when emission systems with a large thermal mass such as Thermally Activated Building Systems (TABS) are applied. In this case, the cost that is minimized is typically a weighted sum of energy use and thermal discomfort.

Although the potential of MPC in building control has been widely demonstrated (Cho & Zaheer-uddin, 2003; Gwerder & Tödtli, 2005; Ihm & Krarti, 2005; Karlsson, 2006; Prívara et al., 2011; Ma et al., 2012; Gyalistras & Gwerder, 2009), the commercial application of MPC in buildings is not widespread. One of the bottlenecks in a reliable application of MPC in real life buildings is deriving an accurate model of that particular building that at the same time is suitable to be applied in the optimal control problem (Morari & Lee, 1999; Dounis & Caraiscos, 2009; Hilliard et al., 2015).

In this paper a comparison is presented between two approaches to derive a building controller model to be used in an MPC for a multi-zone office building. The first approach starts from a detailed first principles dynamic building model which is linearized to obtain a state space controller model (Picard et al., 2015, 2016). In the second approach, measurement data are used to identify a suitable grey-box controller model (Privara et al., 2013). This paper follows the following outline. Several sets of real building data are gathered as validation and identification data. On the one

hand, a detailed dynamic building model (emulator) is validated using these measurement data and is linearized into a state space controller model (further referred as *Lin-Mod*). On the other hand, the same sets of measurement data are used to identify and validate a grey-box model (*IE-Mod*). A last controller model is identified using simulation data instead of the measurement data sets (*IS-Mod*). The simulation data is obtained by a full-year simulation of the emulator using a rule-based controller, to imitate real building operation. The three controller models are compared regarding their prediction performance, after which the MPC performance is evaluated using the same MPC framework but the three different controller models.

2. BUILDING EMULATOR MODEL

This section describes the real multi-zone office building, the building emulator model and the validation of the model using measurement data.

2.1 Description of Building and Building Model.

'Hollandsch Huys', located in Hasselt, Belgium, is an office building with approximately 4000 m^2 of conditioned floor area. The building consists of 5 floors: an underground parking, 3 floors with offices and a rooftop apartment used as private office (Fig. 1). Both landscape and single offices are used in the building. The two main façades are south-west and north-east oriented. The building fulfils all passive house criteria except air tightness (n50=0.99 instead of 0.6).

All transparent parts of the façade are equipped with triple glazing. The window surface lies 40 cm deeper than the façade. Each of them is equipped with an external slat shading device whose angle is adjusted automatically to the solar radiation intensity.

The building is equipped with TABS on the first and second floors. The TABS have a double water piping circuit in each concrete floor. Both circuits can be controlled individually and can be used for heating or cooling. On the ground floor, floor heating is installed, which can only be used for heating. TABS and floor heating cover the major part of the heating and cooling load. The ventilation is used mostly for hygienic purposes. The apartment on the third floor is heated using floor heating and TABS and cooled using the TABS. The heating load is mainly provided by a ground coupled heat pump of 158 kW, while cooling is provided with a direct ground coupled heat exchanger of 72 kW. Reversed heat pump operation for cooling is possible, but has never been used. The Air Handling Unit (AHU) uses a 60 kW gas back up boiler to supply heat in the mid-seasons (spring/autumn) when the building itself is still in cooling mode.

The building is modelled using the open-source Modelica Library IDEAS (Baetens et al., 2015). For a detailed description of its governing equations, we refer to Baetens et al. (2015); Picard et al. (2015). For this study, only the building envelope is considered, i.e. the walls, windows, roofs and TABS. An abstraction is made of the HVAC components, i.e. we assume that 1) the HVAC injects thermal power in the water-circuit of the TABS and 2) all zones have perfectly controllable ventilation supply temperatures. The supply temperature of each zone must, however, be the same. Twelve thermal zones are used to model the three floors as shown in Figure 1. The roof apartment is omitted and the basement is modelled as one extra zone without any control input.

2.2 Validation

A Modelica model of the building is created and validated using real measurement data. The following paragraphs describe the building data, the weather data, the tuning of the model and the model validation.

Measurement data. The Modelica model of the Hollandsch Huys building is validated using 5 sets of measurement data. The first data set was obtained from an experiment conducted on the building during the Christmas holidays of 2012. The building was not or only partially occupied during 11 consecutive days and this opportunity was used to excite the HVAC system with several step inputs: two sequences of whole building cooling down (all HVAC off) and heating up (resp. TABS on and TABS+AHU on), and sequences of active cooling down (TABS cooling on) and heating up (TABS on or TABS+AHU on) of specific zones. These last step inputs are generated to evaluate the intra-zone effect of thermal conditioning. During these experiments, extra zone temperature sensors were installed in

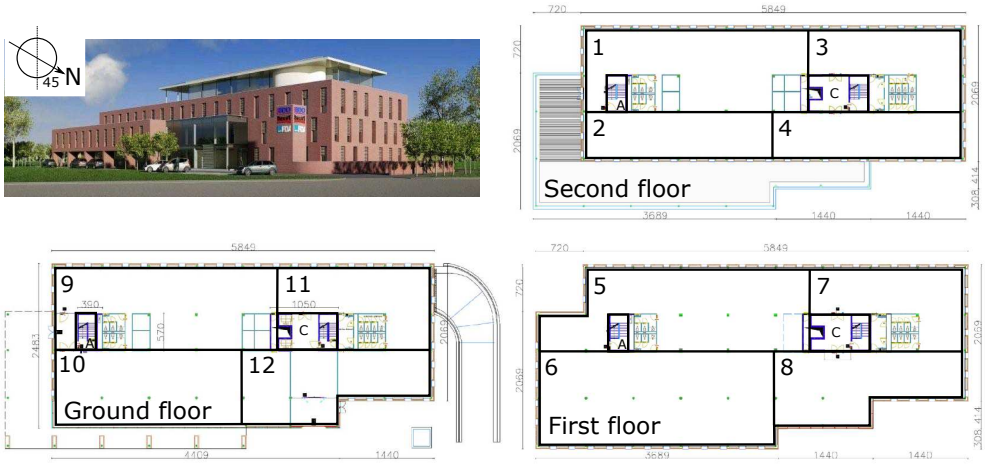

Figure 1: Picture of the *Hollandsch Huys* building and zones layout of the building model.

addition to the Building Management System (BMS) zone temperature sensors, allowing a more accurate validation for each of the 12 zones.

The other four data sets each contain approximately one month of measurement data during the year 2014: Jan 14-Feb 10; May 9-June 2; June 13-July 7; Aug 23-Sept 16. These periods were the only error-free data sets for zones 1, 2 and 4 (Figure 1) and reflect a winter, a mid-season and two summer periods. Due to corruption or failure of many sensors of the BMS, no data during 2014 is available to validate the 9 other zones.

Weather data. The building does not have a local weather station, although during the Christmas experiment the ambient temperature was measured using a dedicated temperature sensor. Therefore, the identification and validation data sets from the BMS are extended with historical data of a weather station in Hasselt obtained from the website `forecast.io`. In order to verify this data, the Christmas ambient temperature from the weather station in Hasselt (F-Hasselt) was compared with those from the airport of Maastricht from both `forecast.io` (F-Maastricht) and `www.wunderground.com` (WG-Maastricht). The comparison shows that the weather data are similar except between the 31st of December and the first of January. The data F-Hasselt is chosen because it is the closest match and because no solar information is available for historical data from `www.wunderground.com`. The direct normal irradiation and the diffuse irradiation on a horizontal surface are computed using the cloud coverage factor from the weather data and the theoretical cloudless solar radiation, which depend on the position of the sun and on the geographical location (*PyEphem*, 2016; Brinsfield et al., 1984). Using this conversion, the ambient temperature, direct normal and diffuse horizontal irradiation are known. The Modelica model then makes a geometrical projection on the building surfaces.

Model parameter tuning and validation results. The data obtained during the Christmas experiment (D-Xmax) are used to fine-tune the Modelica model, while the data sets of the year 2014 (D-Y14) are used as validation data. In order to obtain a good temperature fit on D-Xmax, the following tuning is done: the insulation thickness is increased below the apartment and decreased for all roof surfaces that are not below the roof-apartment. The heat capacity of the TABS concrete is doubled from 840 J/kgK to 1680 J/kgK.

For the validation using D-Y14, the tuning made with D-Xmas is kept unchanged and only the internal gains are reduced by 40% compared to their theoretically estimated values. Figure 2 shows boxplots of the air temperature error for each validated zone. The horizontal line corresponds to the median, the box to the first and third quartiles, the whiskers to the 95% confidence interval and the crosses to the outliers. Figure 2b shows that the errors on the validation data mostly stay below 1 K for the entire data set, which indicates that the Modelica model is a realistic representation of the real building.

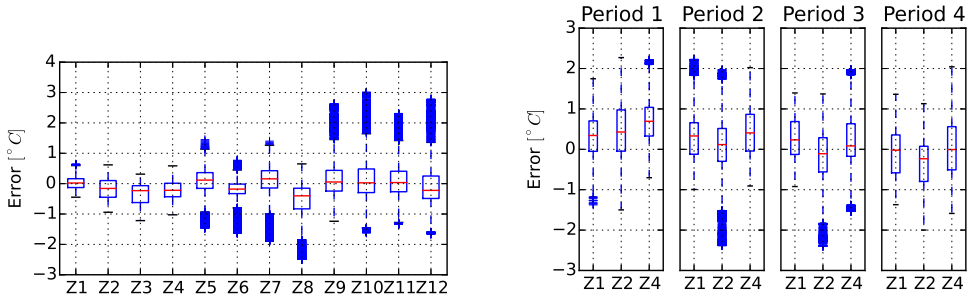

(a) Christmas experiment. **(b) Year 2014.**

Figure 2: Boxplot of the air temperature error for each zone for the tuning data-set (a) and for zones 1, 2 and 4 using the four validation data sets of one month each (b).

3. CONTROLLER MODEL

This section describes the different controller models. Section 3.1 describes the controller model obtained by linearizing the emulator model, Section 3.2 the ones obtained by system identification, and Section 3.3 compares their prediction performance.

3.1 Linearized Controller Model

The heat transfer equations describing the thermal behavior of the building envelope are non-linear. For example, the convection coefficient depends on the wind speed or on the temperature gradient due to buoyancy effect, the radiative heat transfer depends on the temperature to the fourth power and the amount of solar radiation through the windows depends on the solar position, on the shading and on the glass properties. However, the convective and radiative heat transfer equations can be approximated using linear functions and the solar radiation through the windows can be pre-computed since it does not depend on the building states.

In this paper, the building linearization method proposed by Picard et al. (2015) is applied. The authors demonstrated an example where the non-linear building model can be approximated using a linear time-invariant (LTI) State Space Model (SSM) with an error band typically below $\pm 1K$. Using this approach a SSM of 821 states is obtained for the building envelope model of Hollandsch Huys. The SSM inputs are the thermal powers injected in the water circuit of the TABS, the supply ventilation temperature to the zones, the convective and radiative occupancy heat gains, the various ambient conditions, and the solar radiation through each window. Section 3.3 shows that the linearized model is able to predict the zone temperatures of the emulator model with an error mostly smaller than ± 0.1 K.

3.2 Grey-box Controller Model

Grey-box system identification is a technique which pre-defines the model structure based on physical knowledge but which optimizes its parameter values such that the model response fits some measurement data.

In this paper, a method based on the simplified discretization of the continuous model structure is used, as described by Privara et al. (2013) in the *deterministic semi-physical modeling* section of their paper. The method boils down to parameter estimation of a linear SSM. The SSM structure is constructed based on physical knowledge about the building and its discretization is then approximated by its first order Taylor expansion. The model parameters are estimated by solving a quadratic programming problem in which the one step ahead prediction error is minimized and the parameter values are constrained within physically meaningful bounds defined by the user. By keeping the model linear, the identification procedure can be formulated as a convex optimization problem.

In this paper, the model structure corresponds to the so-called RC-model depicted by Fig. 3. The model is composed of thermal resistances (representing thermal conduction, convection and radiation resistances) and capacitances (representing the heat capacity of the building mass). Each zone is represented by 3 nodes (zone temperature $T_{z,i}$, floor concrete temperature $T_{f,i}$, ceiling concrete temperature $T_{c,i}$). The energy delivered by the AHU $\dot{Q}_{AHU,i}$, internal gains

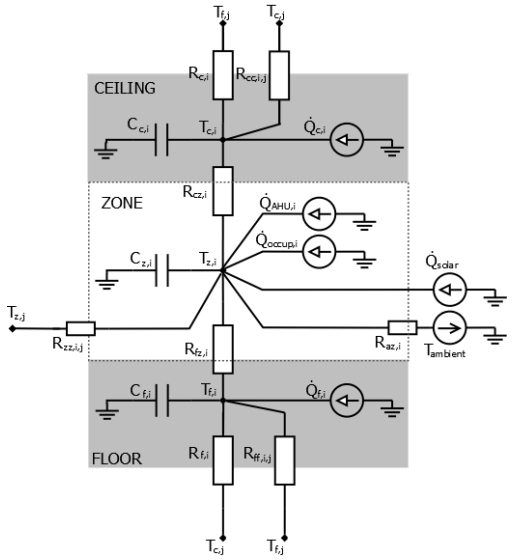

Figure 3: RC network of a zone. Subscripts f,z,c stand for floor, zone, ceiling respectively, and subscripts i and j stand for zone number. T stands for temperature (analogous to voltage) and $\dot{Q}$ stands for heat flux (analogous to electric current). The sources represent the inputs to the model – either temperatures or heat fluxes. Note that subscript j may represent more than one zone – it covers all neighboring zones

from occupants $\dot{Q}_{occup,i}$ and the solar radiation entering the zone through its windows $\dot{Q}_{solar}$ are injected in the zone capacity while the energy delivered to the TABS is injected in the floor and ceiling capacities. Thermal resistances exist between each zone and i) the ambient temperature $T_{ambient}$, ii) all neighboring zones $T_{z,j}$, iii) its ceiling and its floor. Ceilings and floors are coupled both vertically and horizontally to each others.

Two controller models with the same structure are identified: *IS-Mod* is identified using data obtained by simulation using the emulator building with a reference controller from January to July, and *IE-Mod* is identified using D-Xmas. The identification data is sampled every $T_s = 320s$ and the inputs are converted such that all inputs are either expressed in kW or $^\circ C$. This ensures that the estimation problem is not ill-posed. The global solar radiation on the horizontal plane, available in the identification data set, is transformed into solar radiation per façade taking the solar blind into account. Window area and window properties are considered only in the case of identification from real data. For this model, the coupling between neighboring zones is not considered as it increases the number of parameters to estimate and information contained in the identification data is insufficient to identify all parameters correctly.

3.3 Validation of Controller Models

In this section, the controller models are validated against the reference emulator model (*Ref-Mod*). The operative temperatures (i.e. a weighted temperature composed of the air temperature and the zone surface temperatures) of *Ref-Mod* are compared to the values of the linearized model (*Lin-Mod*), the identified model using simulation data (*IS-Mod*), and the identified model using experiment data (*IE-Mod*). The controller models are excited with the same (or the equivalent) inputs as *Ref-Mod*. *Ref-Mod* is simulated over a full year using a typical meteorological year from Uccle, Belgium (Meteotest, 2009) and typical control inputs. The simulation integrator step for *Ref-Mod* is 30 seconds and the outputs are sampled each 900 seconds. The controller models, however, are transformed to discrete SSM with the same sampling time as the MPC ($T_s = 3600$s) and the inputs are sampled accordingly using zero-hold. For model consistency, *IS-Mod* and *IE-Mod* are transformed such that their inputs and outputs are in Watt and Kelvin instead of kilo-Watt and degrees Celsius. Further, as only the global supply ventilation temperature ($T_{sup,ven}$) can be controlled and not the ventilation thermal power to each zone ($\dot{Q}_{ven,i}$), the controller models are extended to use $T_{sup,ven}$ and the nominal ventilation mass flow rates instead of the $\dot{Q}_{ven,i}$'s. As explained in Section 4.1, this transformation introduces a model mismatch for each zone but it becomes zero when the average is taken over all zones.

Figure 4a and 4b show 3-day winter and summer validation sets for the average operative temperature $T_{op,av}$ of the

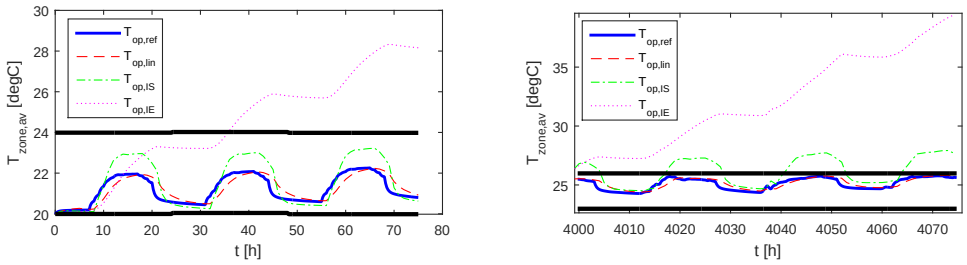

(a) Winter period. **(b) Summer period.**

Figure 4: Average operative temperature of all zones for the reference model ($T_{op,ref}$), the linearized model ($T_{op,lin}$), the identified model using simulation data ($T_{op,IS}$), and the identified model using experiment data ($T_{op,IE}$) for a winter period (a) and for a summer period (b).

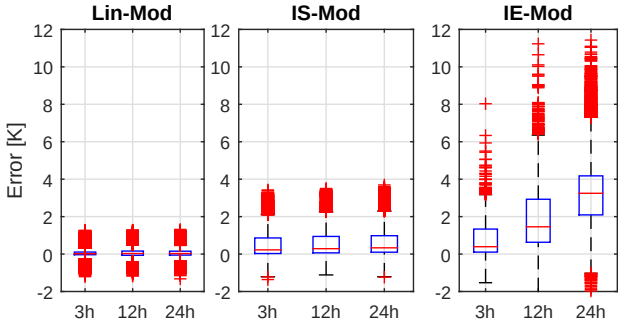

Figure 5: Prediction error for horizons of 3, 12 and 24 hours for the linearized model (*Lin-Mod*), the identified model using simulation data (*IS-Mod*), and the identified model using experiment data (*IE-Mod*).

12 zones. *Lin-Mod* and *IS-Mod* are able to accurately predict $T_{op,av}$. The error made by *Lin-Mod* is mainly due to its zero-hold discretization as decreasing T_s significantly improves the predictions. For the *IS-mod* and *IE-mod*, no operative temperature is available and the temperature of the zone is used instead. This is the main cause of model mismatch for the *IS-mod* as its zone temperatures do coïncide better with the air temperature of the reference model. However, both *IS-mod* and *IE-mod* show a temperature drift causing a serious prediction error for *IE-mod*. The drift probably originates from the system identification procedure which is carried out in the discrete time domain. An estimation error on the parameters can then lead to an integration error, which means the numerical creation of energy within the model. Simulating *IS-Mod* and *IE-Mod* with zero heat inputs and constant temperature input does indeed not result to convergence of the states to the temperature input value.

Figure 5 shows a boxplot of the prediction error of *Lin-Mode*, *IS-Mod* and *IE-Mod* for the prediction horizons of 3, 12 and 24 hours. The prediction errors are obtained by taking 1000 points from the reference simulation, evenly spaced over the whole year. For each point, the controller models are initialized with the corresponding state values of the reference simulation and the temperatures at the end of the prediction horizon are computed. Figure 5 gives the errors between these prediction temperatures and the reference temperatures for all zones together. Figure 5 shows that the *Lin-Mod* predictions are for 95% within ± 0.5 K for all horizons and the average prediction error is zero. The medians for *IS-Mod* and *IE-Mod* are positive which indicates a systematic overestimation of the temperature. However, *IS-Mod* is still able to predict the temperature with an error band of $[0, 1]$ K for 75% of the time. This is not the case for *IE-Mod* which shows an average prediction error of 3 K for a horizon of 24 hours.

4. MPC CONTROLLER

This section describes the MPC formulation and the algorithm and software used to solve the MPC problem.

4.1 MPC cost function, constraints and parameters

In this work, the MPC optimization problem boils down to minimizing the heating and cooling TABS energy ($\mathscr{T}_{H,i}^{(k)}$, $\mathscr{T}_{C,i}^{(k)}$), and the ventilation energy $\mathscr{V}_i^{(k)}$, while the operative zone temperature $T_{op,i}$ stays within the time varying comfort band $[T_{\text{lb}}^{(k)}, T_{\text{ub}}^{(k)}]$ by minimizing the slack variable $\mathscr{S}_c^{(k)}$ (Eq. 1a). The subscript i represents the zone number, H and C refer to heating and cooling and (k) refers to the time step within the MPC horizon of length $N \times T_s$ with T_s the sampling time. The sampling time in this work is 1 hour and the horizon is 1 day. The MPC uses perfect state update every 4 hours. Note that using perfect state updates is not possible in reality as not all states (such as the TABS core-temperature) are measurable and, moreover, sensors are not perfect. In order to limit the influence of the state update, the update only takes place every 4 hours, while the typical sampling time for building measurements is between 5 to 30 minutes.

Eq. 1 formulates the MPC cost function and constraints. The optimization variables are $\mathscr{T}_{H,i}^{(k)}$, $\mathscr{T}_{C,i}^{(k)}$, and the ventilation supply temperature $T_{\text{sup,ven}}$. It should be noted that the current ventilation system imposes nominal ventilation flow for each zone when the building is occupied and zero otherwise. $T_{\text{sup,ven}}$ is furthermore the same for all zones, which means that the $\mathscr{V}_i^{(k)}$ computed by the MPC can not be exactly delivered to each zone. The exact value of $\mathscr{V}_i^{(k)}$'s cannot be formulated in the linear MPC as it is bilinear (multiplication of the time varying ventilation mass flow rate $\dot{m}_{\text{i}}^{(k)}$ with $T_{\text{sup,ven}}$ or $T_{\text{air,i}}$). $\mathscr{V}_i^{(k)}$ is approximated in this MPC by assuming that $\dot{m}_{\text{i}}^{(k)}$ is equal to its nominal value (Eq. 1b) and that the supply temperature equals the average of all air zone temperatures $\bar{T}_{\text{air}}$ when $\dot{m}_{\text{1}}^{(k)}$ is zero (Eq. 1i and 1j). Note that all $\dot{m}_i^{(k)}$ are turned on or off at the same time. This forces the MPC to limit $\mathscr{V}_i^{(k)}$ as much as possible when the ventilation is off as the real ventilation system can then not supply the $\mathscr{V}_i^{(k)}$'s to the zones. Due to this approximation, the MPC makes a prediction error on the amount of ventilation power injected when the ventilation is off. The global cost function and constraints can now be formulated as:

$$J = \min_{T_{\text{sup,ven}}, \mathscr{T}_{H,i}, \mathscr{T}_{C,i}} \sum_{k=0}^{N-1} \left[\sum_{i=1}^{12} \left(\underbrace{\mathscr{T}_{H,i}^{(k)} + \mathscr{T}_{C,i}^{(k)}}_{\text{TABS}} + \underbrace{\mathscr{A}_i^{(k)}}_{\text{Ventilation}} \right) + \underbrace{10^6 \mathscr{S}_c^{(k)}}_{\text{Discomfort}} + \underbrace{10^6 \mathscr{S}_v^{(k)}}_{\text{Soft ven.}} \right] \tag{1a}$$

$$s.t. \quad \mathscr{V}_i^{(k)} = \dot{m}_{\text{nom,i}} c_p \left(T_{\text{sup,ven}} - T_{\text{air},i}^{(k)} \right) \tag{1b}$$

$$\mathscr{A}_i^{(k)} - \mathscr{V}_i^{(k)} > 0 \ , \ \mathscr{A}_i^{(k)} + \mathscr{V}_i^{(k)} > 0 \tag{1c}$$

$$\mathscr{T}_{H,i}^{(k)} > 0 \ , \ \mathscr{T}_{C,i}^{(k)} > 0 \ , \ \mathscr{S}_c^{(k)} > 0 \ , \ \mathscr{S}_v^{(k)} > 0 \tag{1d}$$

$$\sum_{i=1}^{12} \mathscr{T}_{H,i}^{(k)} < \mathscr{T}_{\text{H,nom}} \ , \ \sum_{i=1}^{12} \mathscr{T}_{C,i}^{(k)} < \mathscr{T}_{\text{C,nom}} \ , \ \sum_{i=1}^{12} \mathscr{V}_i^{(k)} < \mathscr{V}_{\text{H,nom}} \ , \ \sum_{i=1}^{12} \mathscr{V}_i^{(k)} > -\mathscr{V}_{\text{C,nom}} \tag{1e}$$

$$\mathscr{T}_{H,i}^{(k)} < \mathscr{T}_{\text{H,i,nom}} \ , \ \mathscr{T}_{C,i}^{(k)} < \mathscr{T}_{\text{C,i,nom}} \tag{1f}$$

$$T_{\text{ub}}^{(k)} - T_{\text{sup,ven}}^{(k)} + \varepsilon + \mathscr{S}_v^{(k)} > 0 \ , \ T_{\text{sup,ven}}^{(k)} - T_{\text{lb}}^{(k)} + \varepsilon + \mathscr{S}_v^{(k)} > 0 \tag{1g}$$

$$T_{\text{ub}}^{(k)} - T_{\text{op},i}^{(k)} + \mathscr{S}_c^{(k)} > 0 \ , \ T_{\text{op},i}^{(k)} - T_{\text{lb}}^{(k)} + \mathscr{S}_c^{(k)} > 0 \tag{1h}$$

$$\frac{\dot{m}_1^{(k)}}{\dot{m}_{\text{nom,1}}} \mathscr{V}_{\text{nom,H,1}} - \dot{m}_{\text{nom,1}} c_p \left(T_{\text{sup}} - \bar{T}_{\text{air}} \right) > 0 \tag{1i}$$

$$-\frac{\dot{m}_1^{(k)}}{\dot{m}_{\text{nom,1}}} \mathscr{V}_{\text{nom,C,1}} + \dot{m}_{\text{nom,1}} c_p \left(T_{\text{sup}} - \bar{T}_{\text{air}} \right) > 0 \tag{1j}$$

$$T_{\text{air}}^{(k)} = f\left(x^0, [T_{\text{sup,ven}}, \mathscr{T}_{H,i}, \mathscr{T}_{C,i}]^{(0)\cdots(k)} \right) \tag{1k}$$

with nominal working condition indicated by subscript *nom*, ventilation mass flow rates $\dot{m}_{\text{i}}^{(k)}$, air heat capacity c_p, maximum TABS powers $\mathscr{T}_{H,max}$, $\mathscr{T}_{C,max}$ and $\bar{T}_{\text{air},i}$ the average of all zone air temperature.

The minimization of $\mathscr{A}_i^{(k)}$ and Eq. 1b and 1c are the linear equivalent to the minimization of $|\mathscr{V}_i^{(k)}|$ with $|\cdot|$ representing

the absolute value. Eq. 1e constraints the total thermal powers such that the nominal production power of the heat pump is not exceeded. Eq. 1f limits the power of each TABS circuit, while Eq. 1g confines $T_{\text{sup,ven}}$ within a band ε broader than the comfort band. The relaxation ε is set to 1 K to avoid a too cold or too warm ventilation air flow. The constraint is furthermore relaxed by the slack variable $\mathscr{S}_v^{(k)}$ to improve the robustness of the algorithm. Finally, Eq. 1k represents the dynamics of the controller SSM.

4.2 Software and algorithm

The tool chain used for implementing the MPC controller is described in detail by Jorissen and Helsen (2016). The first step in the tool chain is to convert a detailed emulator model into a linear state space model and to create a file with pre-computed boundary conditions, as described in section 3.1. The tool chain contains an MPC implementation in Modelica that calls a C++ library that performs the actual computations. This library uses the state space and input data to efficiently (Jorissen & Helsen, 2016) formulate an Optimal Control Problem (OCP) using CasADi (Andersson, 2013). This OCP is solved using the CPLEX Dual Simplex QP solver. The Modelica model periodically calls the library to retrieve the optimal control results and to provide data for the state update algorithm within the controller. These optimal control results are used to provide set points for the building HVAC model, after which the simulation can advance in time. After an integer multiple of the MPC time step the states are updated and the OCP is rerun.

5. RESULTS

The MPC formulation is used with the different controller models to control the building climate during a full year simulation. Fig. 6 shows the average of the 12 operative temperatures as calculated by the emulator for the different MPCs together with the lower and upper indicators temperature bounds. Table 1 summarizes the MPC performance factors for the whole building for each MPC, i.e. the heating and cooling energy used by the TABS (TABS-Heat, TABS-Coo) and the ventilation (AHU-Hea, AHU-Coo) and the total discomfort (DC) together with the minimal and maximal deviation from the comfort range.

Figure 6 and Table 1 show that the *Lin-Mod* MPC is able to keep the operative temperatures within the comfort bounds with only a negligible discomfort of 147 Kh/year and with a punctual maximal deviation of 1 K. The discomfort is mainly due to the model mismatch introduced by Eq. 1b which culminates when the air temperatures differ the most between the zones. When $T_{air,i}$ is higher than $\bar{T}_{\text{air}}$ and the ventilation is turned off (i.e. $\dot{m}_1 = 0$), the MPC constraints set $T_{\text{sup,ven}} = \bar{T}_{\text{air}}$. Eq. 1b becomes then negative and the MPC supposes that zone i is cooled by the ventilation while this is in reality not the case. Nevertheless, the discomfort caused by *Lin-Mod* MPC is only 7% and 0.4% of the discomfort caused by *IS-Mod* MPC and *IE-Mod* MPC, respectively, while its energy use is 41% and 8% of the energy used in the *IS-Mod* and ES-Mod approaches, respectively.

While less energy efficient and comfort are guaranteed, *IS-Mod* MPC still achieves good comfort with only 2064 Kh /year of discomfort (172 Kh / zone / year) and its energy use is only 20% of those of *IE-Mod*. Due to the systematic overestimation of the temperatures as shown by Figure 5, *IS-Mod* MPC is not able to work close to the upper temperature comfort bound and therefore it cools more than necessary. Furthermore, the TABS control signals exhibit (not shown) too fast oscillations between heating and cooling actions which lead to an inefficiency energy supply to the building. This bang-bang behavior is caused by the model mismatch and the linear formulation of the objective function. Adding a smoothing term on the inputs in the cost function as proposed by (Cigler et al., 2013) would probably significantly improve the MPC robustness against its prediction errors and so improve its global performance. Figure 5 also shows that errors on the 3 hours ahead prediction are non-negligible which causes regular discomfort when the MPC operates close to the bounds. The maximum deviation of -1.3 K remains, however, acceptable.

Finally, *IE-Mod* MPC shows poor comfort and a total energy use of 476 MWh while the energy use when the building model is controlled by the original rule-based-controller (not explained in the text) stays below 240 MWh. This confirms that due to the lack of 'rich' measurement data, the identified model *IE-Mod* is not reliable enough to be used in an MPC. The collection of 'rich' data (containing enough information for system identification) in real practice is thus a topic for further research, next to testing these approaches in real buildings.

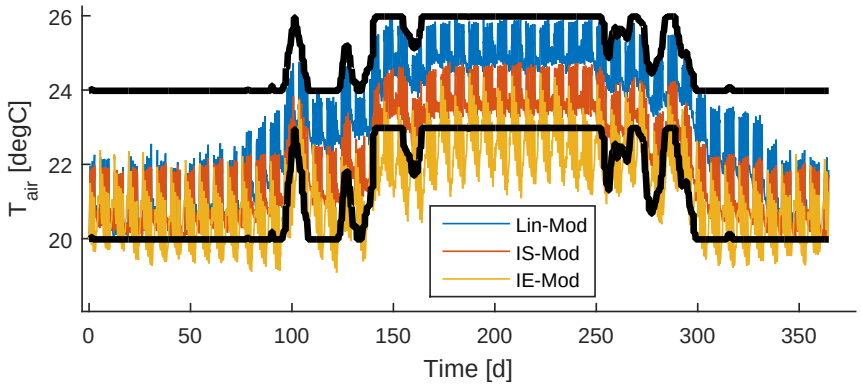

Figure 6: Comparison of the average of all operative zone temperatures for a full year simulation with MPC's using the *Lin-Mod*, the *IS-Mod* and the *IE-Mod* controller models.

Table 1: MPC performance indicators for the three approaches (*Lin-Mod*, *IS-Mod*, *IE-Mod*) in MPC.

	TABS-Heat	TABS-Coo	AHU-Hea	AHU-Coo	DC	Min DC	Max DC
	[kWh_{th} / y]	[kWh_{th} / y]	[kWh_{th} / y]	[kWh_{th} / y]	[Kh / y]	[K]	[K]
Lin-Mod	4360	19931	753	15159	147	-0.4	1.0
IS-Mod	26926	57262	589	14387	2064	-1.3	0.0
IE-Mod	205670	265070	2375	2788	37721	-3.6	0.0

6. CONCLUSION

In this paper, we compared two approaches to obtain a controller model for MPC: a system identification method using a grey-box model approach and a white-box model approach for which a detailed building model is linearized. The MPC performance using both models is evaluated on a validated 12 zones emulator model of an existing office building. The results indicate that the MPC performance is very sensitive to the prediction accuracy of the controller model. This paper shows that both approaches can lead to an efficient MPC as long as very accurate identification data sets are available. For the considered simulation case, the white-box MPC resulted in a better thermal comfort and used only 50% of the energy used by the best grey-box MPC. Tests in real buildings, however, are still needed to confirm the strength of the white-box approach in presence of all uncertainties (weather predictions, state measurement and estimations, user behaviour, ...).

REFERENCES

Andersson, J. (2013). *A General-Purpose Software Framework for Dynamic Optimization* (PhD thesis). Arenberg Doctoral School, KU Leuven, Department of Electrical Engineering (ESAT/SCD) and Optimization in Engineering Center, Kasteelpark Arenberg 10, 3001-Heverlee, Belgium.

Baetens, R., De Coninck, R., Jorissen, F., Picard, D., Helsen, L., & Saelens, D. (2015). OpenIDEAS - An open framework for integrated district energy simulations. In *IPSBA building simulation 2015.* Hyderabad.

Brinsfield, R., Yaramanoglu, M., & Wheaton, F. (1984). Ground level solar radiation prediction model including cloud cover effects. *Solar Energy*, *33*(6), 493–499.

Cho, S., & Zaheer-uddin, M. (2003, May). Predictive control of intermittently operated radiant floor heating systems. *Energy Conversion and Management*, *44*(8), 1333–1342.

Cigler, J., Siroky, J., Korda, M., & Jones, C. (2013). On the selection of the most appropriate mpc problem formulation for buildings. In *11th rehva world congress clima 2013.*

Dounis, A., & Caraiscos, C. (2009, August). Advanced control systems engineering for energy and comfort management in a building environmentA review. *Renewable and Sustainable Energy Reviews*, *13*(6-7), 1246–1261.

Gwerder, M., & Tödtli, J. (2005). Predictive Control for Thermal Storage Management in Buildings. In *8th REHVA world congress for building technologies - CLIMA* (pp. 1–6). Lausanne.

Gyalistras, D., & Gwerder, M. (2009). *Use of weather and occupancy forecasts for optimal building climate control (opticontrol), two years progress report.* (Tech. Rep.). Terrestrial Systems Ecology ETH Zurich.

Hilliard, T., Kavgic, M., & Swan, L. (2015). Model predictive control for commercial buildings: trends and opportunities. *Advances in Building Energy Research*, 1–19.

Ihm, P., & Krarti, M. (2005). Optimal Control Strategies for Heated Radiant Floor Systems. *ASHRAE Transactions*, 535–546.

Jorissen, F., & Helsen, L. (2016). Towards and automated tool chain for MPC in multi-zone buildings, submitted. In *2016 intelligent building operations workshop.* West Lafayette.

Karlsson, H. (2006). *Thermal system analysis of embedded building integrated heating* (Unpublished doctoral dissertation). Chalmers University of Technology.

Ma, Y., Kelman, A., Daly, A., & Borrelli, F. (2012, Feb). Predictive control for energy efficient buildings with thermal storage: Modeling, stimulation, and experiments. *IEEE Control Systems*, *32*(1), 44-64. doi: 10.1109/MCS.2011.2172532

Maciejowski, J. M. (2002). *Predictive Control with Constraints*. Harlow, Essex: Pearson Education Limitedl.

Meteotest. (2009). Meteonorm version 6.1 - edition 2009 [Computer software manual].

Morari, M., & Lee, J. H. (1999). Model predictive control : past , present and future. *Computers & Chemical Engineering Engineering*, *23*, 667–682.

Picard, D., Drgoňa, J., Helsen, L., & Kvasnica, M. (2016). Impact of the plant and controller model complexity on model predictive control performance evaluation for buildings, submitted. *Applied Energy*.

Picard, D., Jorissen, F., & Helsen, L. (2015). Methodology for obtaining linear state space building energy simulation models. In *11th international modelica conference* (pp. 51–58).

Privara, S., Cigler, J., Vana, Z., Oldewurtel, F., Sagerschnig, C., & Zacekova, E. (2013, JAN). Building modeling as a crucial part for building predictive control. *Energy & Buildings*, *56*, 8-22. doi: {10.1016/j.enbuild.2012.10.024}

Prívara, S., Široký, J., Ferkl, L., & Cigler, J. (2011, February). Model predictive control of a building heating system: The first experience. *Energy & Buildings*, *43*(2-3), 564–572.

Pyephem. (2016). `https://pypi.python.org/pypi/pyephem/`. (Accessed: 2016-04-28)

ACKNOWLEDGEMENT

The Authors gratefully acknowledge the financial support of the of the Scientific Grant Agency of the Slovak Republic under the grants 1/0403/15. The authors also acknowledge the financial support by the Agency for Innovation by Science and Technology in Flanders (IWT) and WTCB in the frame of the IWT-VIS Traject SMART GEOTHERM focusing on integration of thermal energy storage and thermal inertia in geothermal concepts for smart heating and cooling of (medium) large buildings, as well as the financial support of the Ph.D. work of Filip Jorissen (IWT 131012 Ph.D. Grant), and the EU for funding the research work of Maarten Sourbron.